A Comparison of Staggered-Grid, Conventional One-step, and Optimally Accurate Finite-Difference Schemes for Computing Synthetic Seismograms

Robert J. Geller

Department of Earth and Planetary Science, Graduate School of Science, University of Tokyo

Hongo 7-3-1, Bunkyo-ku, Tokyo 113-0033, Japan

email: bob@eps.s.u-tokyo.ac.jp

Nobuyasu Hirabayashi

Schlumberger K.K., 2-2-1 Fuchinobe, Sagamihara-shi, Kanagawa-ken 229-0006, Japan

email: nhirabayashi@slb.com

and

Department of Earth and Planetary Science, Graduate School of Science, University of Tokyo,

Hongo 7-3-1, Bunkyo-ku, Tokyo 113-0033, Japan

Hiromitsu Mizutani

Institute for Research on Earth Evolution (IFREE),

Japan Agency of Marine-Earth Science and Technology (JAMSTEC)

Showa-machi 3173-25, Kanazawa-ku, Yokohama 236-0001, Japan

email: miju@jamstec.go.jp

Short title: Comparison of FD Schemes

Revised: May 30, 2006 **Submitted**: October 19, 2005

ABSTRACT

We compare the cost-effectiveness (as quantified by the CPU time required to attain a given level of accuracy) of various finite-difference (FD) schemes for computing synthetic seismograms. Broadly speaking, published FD schemes can be divided into two classes: staggered-grid (SG) schemes, in which velocity and stress are the dependent variables, and schemes in which displacement (or velocity) is the only dependent variable. "Displacement only" schemes can be further divided into conventional one-step FD schemes and optimally accurate FD schemes; the latter have been shown to be about an order of magnitude more cost-effective than the former for one-dimensional (1-D) problems, and two orders of magnitude more efficient for 3-D problems. We show that SG schemes can be transformed into one-step schemes in which velocity is the only dependent variable, thereby allowing a straightforward comparison of SG, conventional one-step, and optimally accurate FD schemes in a common framework. We use this result to show that an SG scheme which is second order in time and fourth order in space, $O(2,4)$, is equivalent to a non-optimally accurate one-step FD scheme with a seven point spatial operator, whereas a conventional $O(2,4)$ one-step FD scheme uses only a five point spatial operator. Thus SG schemes have no advantages in accuracy over conventional one-step FD schemes, while they require more CPU time and memory. In summary, optimally accurate FD schemes significantly outperform both SG schemes and conventional one-step FD schemes. Only homogeneous one-dimensional (1-D) cases are considered in this paper, but the above conclusions also apply to the heterogeneous 1-D, 2-D and 3-D cases.

INTRODUCTION

Extensive research has been conducted on finite-difference (FD) methods for numerically solving the elastic equation of motion (see, e.g., review by Carcione *et al.*, 2002). However, FD methods have heretofore mainly been used to make forward calculations of synthetic seismograms to assist in understanding what types of waves would be produced by a given Earth structure model, rather than to compute synthetics that will be compared quantitatively to observed data to invert for Earth structure. For this reason, FD schemes that produce "reasonable" synthetics seem to have been acceptable to most users, and accurate quantification of the error of synthetic seismograms does not seem to have been widely viewed as an important issue. However, applications which require highly and verifiably accurate synthetics are now becoming more widespread. For example, 3-D reverse-time prestack depth migration (RT PSDM) is now becoming increasingly important in exploration, while waveform inversion for Earth structure is becoming increasingly common in academic research. As these applications require accurate calculations for 3-D Earth models, computational efficiency is essential. A re-examination of FD schemes thus seems timely.

Broadly speaking, published FD schemes can be divided into two classes: staggered-grid (hereafter called SG) schemes, in which velocity and stress are the dependent variables, and schemes in which displacement (or velocity) is the only dependent variable. "Displacement only" schemes can be further divided into conventional one-step FD schemes and optimally accurate FD schemes. As noted by Levander (1988, p. 1425), some conventional one-step FD schemes (e.g., that of Kelly *et al.*, 1976) suffer from some or all of the following problems: (1) instability and/or worsened grid dispersion/anisotropy for high values of Poisson's ratio, (2) difficulty in representing sources, and (3) problems with the boundary conditions at free surfaces or internal boundaries. However,

because the “displacement only” schemes (both conventional and optimally accurate) used in this paper and our other publications on this subject (e.g., Geller and Takeuchi, 1995, 1998; Takeuchi *et al.*, 1996; Takeuchi and Geller, 2000; and Hirabayashi *et al.*, 2006) are based on the weak form of the equation of motion (e.g., Strang and Fix, 1973; Geller and Ohminato, 1994), they do not suffer from these problems for the same reasons that finite element schemes do not suffer from such problems. For example, both the optimally acccurate and conventional FD schemes for heterogeneous 2-D and 3-D media with free surface boundary conditions presented by Takeuchi and Geller (2000) are stable for all values of the Poisson number.

The reasons that many previously published FD schemes have stability problems in handling external and internal boundaries can be explained by a formal error analysis of these schemes. As we have presented a preliminary report on this topic (Mizutani and Geller, 2005) and are now preparing a full paper, we omit further discussion here.

OPTIMALLY ACCURATE OPERATORS

Lax and Wendroff (1964) presented a method for greatly improving the cost-performance ratio of schemes for solving the scalar wave equation. Such schemes have also been presented by, among others, Marfurt (1984), Claerbout (1985, pp. 262–265), Dablain (1986), and Korn (1987). While the above and other such schemes appear to differ in form, Mizutani *et al*. (2000) showed that they are all essentially equivalent. The above schemes are limited to the case of the scalar wave equation. In contrast, as discussed below, the optimally accurate schemes developed by our group, are, unlike the above schemes, also applicable to the full elastic equation of motion.

In order to derive an efficient scheme for the P-SV problem (or the general 3-D problem) we used first principles to derive a general framework for a formal evaluation of the error of numer-

ical solutions, using an eigenfunction expansion. We used this formal error evaluation to derive a general criterion for optimally accurate numerical operators for solving the elastic equation of motion (Geller and Takeuchi, 1995). Note that it is not necessary to know the numerical values of the eigenfrequencies and eigenfunctions in order to use this criterion to design optimally accurate operators. This criterion can be used to derive optimally accurate computational schemes for arbitrarily heterogeneous media; for the case of homogeneous media it is basically equivalent to the minimization of the numerical dispersion of phase velocity. Two additional benefits are obtained by using this criterion to design operators. (1) The error of the numerical solution as a function of grid size (for the particular type of scheme being used) can be estimated before calculations are made, so that the user's accuracy requirements can be met without using an unnecessarily fine grid. (2) The use of this criterion allows stable operators for boundary nodes to be derived in a straightfoward fashion.

Our first applications of the above criterion were to frequency domain calculations (e.g., Geller and Takeuchi, 1995; Takeuchi *et al*., 1996). We then applied this criterion to time-domain calculations to derive optimally accurate $O(2,2)$ FD schemes, i.e. FD schemes which are second order in time and space, for one dimensional (1-D) problems (Geller and Takeuchi, 1998) and 2-D and 3-D problems (Takeuchi and Geller, 2000). We recently also derived (Hirabayashi *et al*., 2006) an optimally accurate $O(2,4)$ time-domain FD scheme, i.e. an FD scheme which is second order in time and fourth order in space. The above optimally accurate schemes can compute synthetic seismograms for arbitrarily located sources with the same accuracy as for sources at nodes using the source representation of Takeuchi and Geller (2003).

Displacement is the only dependent variable in the above optimally accurate time-domain

schemes, which are implemented using a predictor-corrector algorithm. In the predictor step a conventional one-step FD algorithm is used to compute the displacement at the next time step; the corrector step then computes a correction which eliminates the lowest order error of the predictor step. Because they are predictor-correctors, the CPU time for the optimally accurate schemes is about two to three times that of a conventional one-step scheme of the same order, but the improvement in accuracy is substantial, so that the overall improvement in cost-performance (CPU time require to attain a given level of accuracy) is respectively on the order of a factor of ten, fifty, or over one hundred for the 1-D, 2-D, and 3-D cases (Geller and Takeuchi, 1998; Takeuchi and Geller, 2000). For the convenience of readers, the Appendix of this paper presents the difference stencils and a "numerical recipe" for the optimally accurate $O(2,2)$ FD scheme at an interior point of a homogeneous model (after Geller and Takeuchi, 1998).

Most of our work using optimally accurate numerical operators has been in applications to global seismology, where we compute seismograms in a hetereogeneous earth model (usually vertically heterogeneous but laterally homogeneous, but not limited to the laterally homogeneous case). The synthetic seismograms computed using our methods include both body-waves and surface-waves. We have been using these methods for over ten years to make calculations in heterogeneous Earth models (e.g., Takeuchi *et al.*, 1996; Kawai *et al.*, 2006), and have presented extensive verification and validation exercises. Although the length scale in global seismology is greater than in exploration, the physics of the problem is essentially the same.

STAGGERED-GRID SCHEMES

Staggered-grid (SG) FD schemes appear to be the most widely used methods for numerical computation of synthetic seismograms by the exploration community. In SG schemes, the elas-

tic equation of motion is written as a system of coupled first order partial differential equations (p.d.e.'s), with stress and velocity (rather than displacement) as the two sets of dependent variables. SG schemes then discretize and solve these first order p.d.e.'s using FD techniques. The most significant works on SG schemes (Virieux, 1984, 1986: Levander, 1988) were all published in *Geophysics*. It appears that SG schemes are widely thought to be preferable to other FD schemes. For example, Carcione *et al*. (2002, p. 1308-1309) commented as follows:

> "Staggered grid effectively halves the grid spacing, increasing the accuracy of the approximation.... Staggered grids improve accuracy and stability...."

In this paper we evaluate SG schemes. We first show that SG schemes can be transformed into rigorously equivalent one-step FD schemes, whose computational requirements are somewhat greater than conventional one-step FD schemes, particularly for the case of $O(2,4)$ SG schemes. We next show that the performance of optimally accurate FD schemes is superior to that of conventional one-step FD schemes. Thus optimally accurate FD schemes should be used in preference to either conventional one-step FD schemes or SG schemes.

Analysis of SG schemes

We consider a 1-D problem where u is the displacement,

$$v = u_{,t} \tag{1}$$

is the velocity,

$$\tau = \mu u_{,x} \tag{2}$$

is the stress, f is the body force, ρ is the density, μ is the elastic constant, x is the spatial coordinate,

and t is time. We write the spatial and temporal partial derivatives as $u_{,x}$ and $u_{,t}$, respectively. The strong form of the equation of motion is:

$$(\mu u_{,x})_{,x} - \rho u_{,tt} = -f. \tag{3}$$

On the other hand, by using velocity v and stress τ as the dependent variables, the following two coupled first order p.d.e.'s that serve as the basis for SG schemes are obtained:

$$\tau_{,t} = \mu v_{,x} \tag{4}$$

$$\tau_{,x} = \rho v_{,t} - f. \tag{5}$$

Note that we obtained eq. (4) by taking the time derivative of both sides of eq. (2) and then using eq. (1). We obtained eq. (5) by substituting eqs. (1) and (2) into eq. (3).

If we differentiate eqs. (4) and (5) with respect to x and t respectively, we obtain the following two equations which both have the same left hand sides (l.h.s.):

$$\tau_{,tx} = (\mu v_{,x})_{,x}. \tag{6}$$

$$\tau_{,tx} = \rho v_{,tt} - f_{,t} \tag{7}$$

By equating the right hand sides (r.h.s.) of eqs. (6) and (7) we obtain the following relation, which is the time derivative of eq. (3):

$$(\mu v_{,x})_{,x} - \rho v_{,tt} = -f_{,t}. \tag{8}$$

It is purely a matter of convenience whether we use eq. (3), or eq. (8), or the coupled system of eqs. (4) and (5), as they are equivalent. The above manipulations are trivial, but, as we show below, they provide a roadmap for clarifying the nature of SG schemes.

For the remainder of this paper we consider a homogeneous medium (i.e., μ and ρ are constants) with periodic boundary conditions.

$O(2,2)$ SG scheme

We now consider the standard $O(2,2)$ SG scheme (abbreviated hereafter as SG-2). We begin with the discretized versions of eq. (5) centered around the points $(t+\Delta t/2,x)$ and $(t-\Delta t/2,x)$ respectively. We have:

$$\frac{1}{\Delta x}[\tau(t+\Delta t/2,x+\Delta x/2)-\tau(t+\Delta t/2,x-\Delta x/2)] = \frac{\rho}{\Delta t}[v(t+\Delta t,x)-v(t,x)]-f(t+\Delta t/2,x) \quad (9)$$

$$\frac{1}{\Delta x}[\tau(t-\Delta t/2,x+\Delta x/2)-\tau(t-\Delta t/2,x-\Delta x/2)] = \frac{\rho}{\Delta t}[v(t,x)-v(t-\Delta t,x)]-f(t-\Delta t/2,x). \quad (10)$$

We now subtract eq. (10) from eq. (9) and divide both sides by Δt to obtain the SG-2 counterpart to eq. (7):

$$\begin{aligned}&\frac{1}{\Delta x\Delta t}[\tau(t+\Delta t/2,x+\Delta x/2)-\tau(t+\Delta t/2,x-\Delta x/2)-\tau(t-\Delta t/2,x+\Delta x/2)\\&+\tau(t-\Delta t/2,x-\Delta x/2)]=\frac{\rho}{\Delta t^2}[v(t+\Delta t,x)-2v(t,x)+v(t-\Delta t,x)]\\&-\frac{1}{\Delta t}[f(t+\Delta t/2,x)-f(t-\Delta t/2,x)].\end{aligned} \quad (11)$$

We next consider the discretized versions of eq. (4) centered around the points $(t,x+\Delta x/2)$ and $(t,x-\Delta x/2)$ respectively. We have

$$\frac{1}{\Delta t}[\tau(t+\Delta t/2,x+\Delta x/2)-\tau(t-\Delta t/2,x+\Delta x/2)] = \frac{\mu}{\Delta x}[v(t,x+\Delta x)-v(t,x)] \quad (12)$$

$$\frac{1}{\Delta t}[\tau(t+\Delta t/2,x-\Delta x/2)-\tau(t-\Delta t/2,x-\Delta x/2)] = \frac{\mu}{\Delta x}[v(t,x)-v(t,x-\Delta x)]. \quad (13)$$

We now subtract eq. (13) from eq. (12) and divide both sides by Δx to obtain the SG-2 counterpart to eq. (6):

$$\frac{1}{\Delta x \Delta t}[\tau(t+\Delta t/2, x+\Delta x/2) - \tau(t+\Delta t/2, x-\Delta x/2) - \tau(t-\Delta t/2, x+\Delta x/2) + \tau(t-\Delta t/2, x-\Delta x/2)] = \frac{\mu}{\Delta x^2}[v(t, x+\Delta x) - 2v(t,x) + v(t, x-\Delta x)]. \quad (14)$$

As the l.h.s. of eqs. (11) and (14) are identical, it follows that their respective r.h.s. are also equal. We thus obtain the SG-2 counterpart to eq. (8):

$$\begin{aligned} & \frac{\rho}{\Delta t^2}[v(t+\Delta t, x) - 2v(t,x) + v(t-\Delta t, x)] - \frac{1}{\Delta t}[f(t+\Delta t/2, x) - f(t-\Delta t/2, x)] \\ = \quad & \frac{\mu}{\Delta x^2}[v(t, x+\Delta x) - 2v(t,x) + v(t, x-\Delta x)]. \end{aligned} \quad (15)$$

We refer to this scheme as CSG-2 in our numerical example, because it is the one-step counterpart to SG-2.

Let us now compare eq. (15) to the well known conventional one-step $O(2,2)$ FD scheme (e.g., Geller and Takeuchi, 1998), hereafter called CONV-2, which is as follows:

$$\begin{aligned} & \frac{\rho}{\Delta t^2}[u(t+\Delta t, x) - 2u(t,x) + u(t-\Delta t, x)] - f(t,x) \\ = \quad & \frac{\mu}{\Delta x^2}[u(t, x+\Delta x) - 2u(t,x) + u(t, x-\Delta x)]. \end{aligned} \quad (16)$$

Ignoring the differences in the force term, eq. (15), which, as we showed above, is strictly equal to SG-2, is just the time derivative of CONV-2 (eq. 16). This means that SG-2 schemes are not different in any fundamental way from CONV-2 schemes. Functionally (except for the handling of the force term) the SG-2 scheme is identical to a one-step CONV-2 scheme (but with velocity rather than displacement as the dependent variable) that explicitly defines certain intermediate quantities as named variables which are stored in memory and then almost immediately thereafter retrieved,

used, and discarded. (A similar observation was also made by Luo and Schuster, 1990.) Thus no improvement in accuracy is obtained by using SG-2 rather than CONV-2, while CPU time and memory requirements are slightly increased. This is confirmed by numerical tests, below.

O(2,4) SG scheme

We now consider the standard $O(2,4)$ SG scheme, which we hereafter abbreviate as SG-4. We begin with the discretized versions of eq. (5) centered around the points $(t+\Delta t/2,x)$ and $(t-\Delta t/2,x)$ respectively. We have

$$\frac{1}{\Delta x}\left[-\frac{1}{24}\tau(t+\Delta t/2,x+3\Delta x/2)+\frac{9}{8}\tau(t+\Delta t/2,x+\Delta x/2)-\frac{9}{8}\tau(t+\Delta t/2,x-\Delta x/2)\right.$$
$$\left.+\frac{1}{24}\tau(t+\Delta t/2,x-3\Delta x/2)\right]=\frac{\rho}{\Delta t}[v(t+\Delta t,x)-v(t,x)]-f(t+\Delta t/2,x) \tag{17}$$

$$\frac{1}{\Delta x}\left[-\frac{1}{24}\tau(t-\Delta t/2,x+3\Delta x/2)+\frac{9}{8}\tau(t-\Delta t/2,x+\Delta x/2)-\frac{9}{8}\tau(t-\Delta t/2,x-\Delta x/2)\right.$$
$$\left.+\frac{1}{24}\tau(t-\Delta t/2,x-3\Delta x/2)\right]=\frac{\rho}{\Delta t}[v(t,x)-v(t-\Delta t,x)]-f(t-\Delta t/2,x) \tag{18}$$

We now subtract eq. (18) from eq. (17) and divide both sides by Δt to obtain the SG-4 counterpart to eq. (7):

$$\frac{1}{\Delta x\Delta t}\left[-\frac{1}{24}\tau(t+\Delta t/2,x+3\Delta x/2)+\frac{9}{8}\tau(t+\Delta t/2,x+\Delta x/2)-\frac{9}{8}\tau(t+\Delta t/2,x-\Delta x/2)\right.$$
$$+\frac{1}{24}\tau(t+\Delta t/2,x-3\Delta x/2)+\frac{1}{24}\tau(t-\Delta t/2,x+3\Delta x/2)-\frac{9}{8}\tau(t-\Delta t/2,x+\Delta x/2)$$
$$\left.+\frac{9}{8}\tau(t-\Delta t/2,x-\Delta x/2)-\frac{1}{24}\tau(t-\Delta t/2,x-3\Delta x/2)\right]$$
$$=\frac{\rho}{\Delta t^2}[v(t+\Delta t,x)-2v(t,x)+v(t-\Delta t,x)]-\frac{1}{\Delta t}[f(t+\Delta t/2,x)-f(t-\Delta t/2,x)]. \tag{19}$$

We next consider the discretized versions of eq. (4) centered around the points $(t,x+3\Delta x/2)$, $(t,x+\Delta x/2)$, $(t,x-\Delta x/2)$, and $(t,x-3\Delta x/2)$, respectively. We have

$$\frac{1}{\Delta t}[\tau(t+\Delta t/2,x+3\Delta x/2)-\tau(t-\Delta t/2,x+3\Delta x/2)]$$

$$= \frac{\mu}{\Delta x}\left[-\frac{1}{24}v(t,x+3\Delta x)+\frac{9}{8}v(t,x+2\Delta x)-\frac{9}{8}v(t,x+\Delta x)+\frac{1}{24}v(t,x)\right] \tag{20}$$

$$\frac{1}{\Delta t}[\tau(t+\Delta t/2,x+\Delta x/2)-\tau(t-\Delta t/2,x+\Delta x/2)]$$
$$= \frac{\mu}{\Delta x}\left[-\frac{1}{24}v(t,x+2\Delta x)+\frac{9}{8}v(t,x+\Delta x)-\frac{9}{8}v(t,x)+\frac{1}{24}v(t,x-\Delta x)\right] \tag{21}$$

$$\frac{1}{\Delta t}[\tau(t+\Delta t/2,x-\Delta x/2)-\tau(t-\Delta t/2,x-\Delta x/2)]$$
$$= \frac{\mu}{\Delta x}\left[-\frac{1}{24}v(t,x+\Delta x)+\frac{9}{8}v(t,x)-\frac{9}{8}v(t,x-\Delta x)+\frac{1}{24}v(t,x-2\Delta x)\right] \tag{22}$$

$$\frac{1}{\Delta t}[\tau(t+\Delta t/2,x-3\Delta x/2)-\tau(t-\Delta t/2,x-3\Delta x/2)]$$
$$= \frac{\mu}{\Delta x}\left[-\frac{1}{24}v(t,x)+\frac{9}{8}v(t,x-\Delta x)-\frac{9}{8}v(t,x-2\Delta x)+\frac{1}{24}v(t,x-3\Delta x)\right]. \tag{23}$$

We now multiply eqs. (20), (21), (22), and (23) by weights of $-1/24$, $9/8$, $-9/8$, and $1/24$ respectively, add the four weighted equations, and divide both sides of the resulting equation by Δx to obtain the SG-4 counterpart of eq. (6):

$$\begin{aligned}
&\frac{1}{\Delta x\Delta t}\left[-\frac{1}{24}\tau(t+\Delta t/2,x+3\Delta x/2)+\frac{9}{8}\tau(t+\Delta t/2,x+\Delta x/2)-\frac{9}{8}\tau(t+\Delta t/2,x-\Delta x/2)\right.\\
&+\frac{1}{24}\tau(t+\Delta t/2,x-3\Delta x/2)+\frac{1}{24}\tau(t-\Delta t/2,x+3\Delta x/2)-\frac{9}{8}\tau(t-\Delta t/2,x+\Delta x/2)\\
&\left.+\frac{9}{8}\tau(t-\Delta t/2,x-\Delta x/2)-\frac{1}{24}\tau(t-\Delta t/2,x-3\Delta x/2)\right]\\
=\ &\frac{\mu}{576\Delta x^2}[v(t,x+3\Delta x)-54v(t,x+2\Delta x)+783v(t,x+\Delta x)-1460v(t,x)\\
&+783v(t,x-\Delta x)-54v(t,x-2\Delta x)+v(t,x-3\Delta x)].
\end{aligned} \tag{24}$$

As the l.h.s. of eqs. (19) and (24) are identical, it follows that the respective r.h.s. are also equal. We thus obtain the SG-4 counterpart of eq. (8):

$$\frac{\rho}{\Delta t^2}[v(t+\Delta t,x)-2v(t,x)+v(t-\Delta t,x)]-\frac{1}{\Delta t}[f(t+\Delta t/2,x)-f(t-\Delta t/2,x)]$$

$$
\begin{aligned}
&= \frac{\mu}{576\Delta x^2}\left[v(t,x+3\Delta x) - 54v(t,x+2\Delta x) + 783v(t,x+\Delta x) - 1460v(t,x)\right.\\
&\left.+783v(t,x-\Delta x) - 54v(t,x-2\Delta x) + v(t,x-3\Delta x)\right]\\
&= \frac{\mu}{\Delta x^2}\left\{\frac{1}{64}\left[\frac{1}{9}\left(v(t,x+3\Delta x) - 2v(t,x) + v(t,x-3\Delta x)\right)\right]\right.\\
&-\frac{24}{64}\left[\frac{1}{4}\left(v(t,x+2\Delta x) - 2v(t,x) + v(t,x-2\Delta x)\right)\right]\\
&\left.+\frac{87}{64}\left[v(t,x+\Delta x) - 2v(t,x) + v(t,x-\Delta x)\right]\right\}. \qquad (25)
\end{aligned}
$$

The above result shows that SG-4 is rigorously equivalent to a one-step scheme with a seven point spatial operator, which we refer to as CSG-4, because it is the one step counterpart to SG-4. Note that the last three lines of eq. (25) have been rewritten to show that CSG-4 is, in effect, achieving fourth order accuracy by summing three different operators for the second derivative with weights of 1/64, -24/64, and 87/64 respectively. As we show below (see eq. 27), despite using a seven point operator, CSG-4 achieves only fourth order accuracy. However, as shown below by eqs. (26) and (28), a five point operator is sufficient to achieve fourth order accuracy, so the seven point operator in eq. (25) is unnecessary. Omitting intermediate steps, note that if the three weights in eq. (25), namely $1/64$, $-24/64$, and $87/64$, were replaced by weights of 1/10, -6/10, and 15/10 respectively, sixth order accuracy would be obtained. However, there is no obvious way to change the derivation of the SG-4 scheme to obtain the latter set of weights.

In contrast to eq. (25), the conventional $O(2,4)$ one-step FD scheme (e.g., Hirabayashi *et al.*, 200), hereafter called CONV-4, is as follows:

$$
\begin{aligned}
&\frac{\rho}{\Delta t^2}\left[u(t+\Delta t,x) - 2u(t,x) + u(t-\Delta t,x)\right] - f(t,x)\\
&= \frac{\mu}{12\Delta x^2}\left[-u(t,x+2\Delta x) + 16u(t,x+\Delta x) - 30u(t,x) + 16u(t,x-\Delta x) - u(t,x-2\Delta x)\right]\\
&= \frac{\mu}{\Delta x^2}\left\{-\frac{1}{3}\left[\frac{1}{4}\left(u(t,x+2\Delta x) - 2u(t,x) + u(t,x-2\Delta x)\right)\right]\right.
\end{aligned}
$$

$$+\frac{4}{3}\left[u(t,x+\Delta x)-2u(t,x)+u(t,x-\Delta x)\right]\Bigg\}. \tag{26}$$

Note that the last two lines of eq. (26) have been rewritten to show that CONV-4 is, in effect, achieving fourth order accuracy by summing two different operators for the second derivative with weights of -1/3 and 4/3 respectively.

If we expand the SG-4 spatial operator (the r.h.s. of eq. 25) in a Taylor series we obtain:

$$\text{r.h.s. of eq (25)} = \mu\left(\frac{\partial^2 v}{\partial x^2} - \frac{3\Delta x^4}{320}\frac{\partial^6 v}{\partial x^6} + \cdots\right). \tag{27}$$

Thus the error is $O(\Delta x^4)$. On the other hand, if we expand the CONV-4 spatial operator (the r.h.s of eq. 26) in a Taylor series we obtain:

$$\text{r.h.s. of eq (26)} = \mu\left(\frac{\partial^2 u}{\partial x^2} - \frac{\Delta x^4}{90}\frac{\partial^6 u}{\partial x^6} + \cdots\right), \tag{28}$$

so the error of CONV-4 is thus also $O(\Delta x^4)$.

In summary, SG-4 has the following two significant drawbacks: first, it effectively uses a seven point spatial operator (eq. 25), rather than the five point operator needed by CONV-4 (eq. 26), to compute a quantity that is only accurate to fourth order; second, it entails needless overhead for defining, computing, and storing, and then almost immediately thereafter retrieving, using and discarding intermediate quantities. The use of SG-4 as opposed to CONV-4 (or the use of SG-2 as opposed to CONV-2) is thus contra-indicated. This is confirmed below by numerical tests. However, we also show below that optimally accurate schemes should in turn be preferred to either CONV-2, SG-2, CONV-4, or SG-4.

STABILITY AND NUMERICAL DISPERSION

In order to determine the stability condition and numerical dispersion of phase velocity for each type of FD scheme we perform a standard von Neumann analysis, in which we substitute a solution of the form $u = \exp(i\omega\Delta t)\exp(ik\Delta x)$ into the FD equations. The stability limit is expressed by the Courant parameter, C, which is defined as follows:

$$C = \beta\Delta t/\Delta x, \tag{29}$$

where the velocity of wave propagation is

$$\beta = \sqrt{\mu/\rho}. \tag{30}$$

The stability limit for each scheme is the maximum value of C for which $A = \cos\omega\Delta t$ is real and for which $-1 \leq A \leq 1$ for all $-1 \leq E \leq 1$, where $E = \cos k\Delta x$. We also define $F = \cos 2k\Delta x$, $G = \cos 3k\Delta x$, and $H = \cos 4k\Delta x$, which are used below.

In addition to the stability limit, another key parameter is the numerical dispersion of the phase velocity for each scheme, which is defined to be:

$$\beta_{num} = \omega/k. \tag{31}$$

Eq. (31) can be used to derive both exact expressions for β_{num} and approximate expressions for small values of $k\Delta x$.

We present results for numerical dispersion for SG-2, SG-4, CONV-2, and CONV-4, which are discussed above, OPT-2 (the optimally accurate $O(2,2)$ predictor-corrector scheme of Geller

and Takeuchi, 1998), and OPT-4 (the optimally accurate $O(2,4)$ predictor-corrector scheme of Hirabayashi *et al*., 2006). Appendix B of Hirabayashi *et al*. (2006) gives analytic results for the stability limit and numerical dispersion for CONV-2, CONV-4, OPT-2, and OPT-4. As shown above, the numerical dispersion and stability limit of SG-2 will be identical to that of CONV-2. Following Hirabayashi *et al*. (2006), and omitting intermediate steps, we obtain the following dispersion relation and stability limit for SG-4:

$$C \leq \sqrt{36/49} \approx 0.857 \tag{32}$$

$$2A-2 = (C^2/576)(2G-108F+1566E-1460) \tag{33}$$

$$\begin{aligned} \beta_{SG4} &= [1/(k\Delta t)]\,\cos^{-1}\left[1+(C^2/576)\,(-730+783E-54F+G)\right] \\ &\approx \beta\left(1+C^2k^2\Delta x^2/24+\cdots\right) \end{aligned} \tag{34}$$

We summarize the stability limits and lowest order numerical dispersion of phase velocity in Table 1. The exact dispersion relations for the various schemes are given in Table 2. Table 1 shows that the numerical dispersion of SG-2/CONV-2, CONV-4, and SG-4 is $O(\Delta x^2)$, while OPT-2 and OPT-4 have errors of $O(\Delta x^4)$. It might surprise some readers that some schemes with a fourth order spatial operator (CONV-4, SG-4) have $O(\Delta x^2)$ numerical dispersion, while a scheme with a second order spatial operator (OPT-2) has $O(\Delta x^4)$ numerical dispersion. However, the explanation is simple (see Hirabayashi *et al*., 2006 for details). The order of error of the numerical dispersion is controlled by the cancellation (or non-cancellation) of the respective errors of the spatial and temporal operators, rather than by the individual error of each of these operators. The optimally accurate schemes are derived using the criterion of Geller and Takeuchi (1995), which minimizes

the numerical dispersion of phase velocity by defining the spatial and temporal operators so that their errors cancel to lowest order.

Results for the numerical dispersion of the phase velocity for four different values of the Courant number ($C = 0.1$, 0.3, 0.5, and 0.8) are shown in Fig. 1. The horizontal axis of each panel of Fig. 1 is the grid parameter (the reciprocal of the number of grid points per wavelength), defined by

$$\text{Grid parameter} = \Delta x/\lambda = k\Delta x/(2\pi), \tag{35}$$

where λ is the wavelength. The vertical axis in each panel of Fig. 1 is the percentage error of the phase velocity, computed using the exact equations in Table 2. The error of CONV-2 (and that of SG-2, which is rigorously equal to CONV-2) is the largest among all the schemes in the first three panels, but is somewhat smaller that that of CONV-4 and SG-4 in the last ($C = 0.8$) panel. Note that as C increases, the error of CONV-2 (and SG-2) decreases, which is fully consistent with the factor of $(1 - C^2)$ in Table 1. In contrast, the error of CONV-4 and SG-4 changes signs as C increases from 0.1 to 0.5, and further increases in magnitude as C increases to 0.8. The performance of SG-4 and CONV-4 is almost identical, which is expected on the basis of the fact that, as shown in Table 1, the errors are the same to lowest order, but SG-4 is slightly worse. The difference between CONV-4 and SG-4 decreases as C increases. It is notable that OPT-2 and OPT-4 significantly outperform the other schemes for $C = 0.5$ and 0.8.

The question of how much accuracy is required depends on each user's need for each particular application. However, in actual travel time data, a difference of 0.1 percent (5 ms in 5 s in exploration, or 1 s in 1000 s in global studies) can definitely be resolved. Thus if we want to compare FD synthetics to real data we will probably require a numerical dispersion error which is about one or-

der of magnitude smaller, namely 0.01 percent. The horizontal scale in panels (c) and (d) of Fig. 1 shows that even OPT-2 and OPT-4 require about 20-25 grid points per wavelength to reach this level of accuracy, while the other schemes require on the order of 100 grid points per wavelength. Of course if the user decides that a lesser level of accuracy is acceptable a commensurately lower value of the grid parameter can be used.

TRADEOFF BETWEEN ACCURACY AND CPU TIME

As the error of the numerical phase velocity can be defined only for a homogeneous medium, we need a measure of accuracy that can be used for an arbitrarily hetereogeneous model. We use the relative solution error (expressed as a percentage), defined as follows:

$$\text{relative r.m.s. error} = 100 \times \left(\frac{\sum_{i=1}^{N} (u_i^j - [u^{(0)}]_i^j)^2}{\sum_{i=1}^{N} ([u^{(0)}]_i^j)^2} \right)^{1/2}, \tag{36}$$

where N is the number of nodes, u_i^j is the calculated displacement at the ith node at the jth time step, and $[u^{(0)}]_i^j$ is the reference displacement at the ith node at the jth time step. Geller and Takeuchi (1995) showed that if the eigenfrequencies of the normal modes of vibration were to be calculated using optimally accurate operators—i.e., operators designed to minimize the relative solution error—the error of the calculated eigenfrequencies would also be minimized. Thus the criterion of minimization of the relative solution error is the logical extension to the case of a heterogeneous medium of the criterion of minimization of phase velocity dispersion for a homogeneous medium.

In the numerical examples in this paper we use the exact (analytic) solution as the reference displacement, but for heterogeneous models a numerical solution obtained with a fine spatial grid

and a small time step can be used. In this paper we use the data at the final time step in evaluating eq. (36). Because data from all grid points are used in our evaluation of eq. (36), a robust measure of accuracy is obtained.

The most important datum to the user is not the grid parameter required to achieve a given level of accuracy, but rather the CPU time required. We now consider the performance of the various numerical schemes discussed in this paper for the case of a 1-D homogeneous medium with a length of 3 km and with periodic boundary conditions. The wave propagation velocity is $\beta = 2$ km/s, and the density is $\rho = 1000$ kg/m^3. The final time step is t=11.5 s in all calculations. The purpose of this numerical test is not to present a detailed evaluation of all of the methods discussed in this paper, but rather to show that SG schemes are marginally inferior to conventional one-step FD schemes, and are considerably inferior to optimally accurate FD schemes.

Results for four different Courant numbers are shown in Fig. 2. In addition to the schemes shown in Fig. 1, we also present results for the one-step counterpart scheme to SG-2 (CSG-2, eq. 15) and the one-step counterpart scheme to SG-4 (CSG-4, eq. 25). We present results for the same four values of the Courant number shown in Fig. 1. The best performing schemes are those that require the least CPU time to achieve a given level of accuracy, or, equivalently, those which achieve the most accurate calculations for a given expenditure of CPU time. Thus the best performing schemes are those whose curves lie closest to the lower left-hand corner of each panel. In all cases the optimally accurate schemes outperform all of the non-optimally accurate schemes by a substantial margin. As expected from the basic equivalence of CSG-2, SG-2 and CONV-2, the performance of these schemes is almost the same. This is also the case for CSG-4, SG-4 and CONV-4.

For the case of $C = 0.5$, for example (Fig. 2c), the OPT schemes achieve a 100-fold improvement in accuracy for a comparable expenditure of CPU time. The results of Geller and Takeuchi (1998) and Takeuchi and Geller (2000) show that the improvement factor for 2-D or 3-D will be considerably greater than that for 1-D, although the numerical values will always depend on the details of the test. Such significant factors of improvement in the cost-performance ratio suggest that it is worthwhile to make the investment in developing and using optimally accurate FD codes in cases where accuracy of the calculations is an important issue. As the results in Fig. 2 are based on the error at the final time step, whereas those in the above cited papers were based on the average error throughout the time window of the synthetics, the numerical values of the improvement factors reported here are somehat larger.

If taken at face value, Fig. 2 appears to show that OPT-4 is preferable to OPT-2. However, the results in Fig. 2 are for the case of a homogeneous model, whereas real FD calculations will always be made for a heterogeneous model with sharp lithological discontinuities. Hirabayashi *et al.* (2006) have conducted 1-D evaluations for models with sharp lithological discontinuities, and have shown that for such cases the boundary error of the OPT-4 operators is quite large. As a result, OPT-2 outperforms OPT-4 for such cases. The ease of programming an OPT-2 scheme, as compared to OPT-4, and the ability of OPT-2 to handle inter-node lithological discontinuities (Mizutani, 2001) also argue in favor of OPT-2. In any case, it seems clear that optimally accurate schemes should be used in preference to non-optimally accurate schemes.

APPLICABILITY TO HETEROGENEOUS PROBLEMS

Since the primary applications of numerical methods for computing synthetic seisimograms are for heterogeneous media in 2-D and 3-D, we discuss the applicability of the above results to such

problems. We also present a numerical example showing the application of optimally accurate FD schemes to a realistic 2-D case.

First, let us consider how SG schemes for a general heterogeneous medium can be transformed, by a trivial extension of the above derivation, to eliminate stress, thereby obtaining a scheme in which the displacement is the only dependent variable. The key point to the derivation is that for the heterogeneous 2-D and 3-D cases, as for the homogeneous 1-D case, the spatial and temporal derivatives of the stress appear without being multiplied by elastic constants (just as they do in the differential equations, eqs. 4 and 5, or the FD equations, eqs. 9, 10, 12, and 13). That being the case, stress can be readily eliminated by taking additional finite differences, as is done above, to obtain a counterpart FD scheme, in which displacement is the only dependent variable. Such counterpart FD schemes have a different form than eqs. (15) or (25), but are basically the same. The exact form of the counterpart FD scheme is not particularly important. Rather what is important is that the counterpart schemes can readily be shown not to satisfy the criterion for optimally accurate FD operators (Geller and Takeuchi, 1995).

In contrast, the scheme presented by Takeuchi and Geller (2000) allows optimally accurate calculations to be made for an arbitrarily heterogeneous elastic medium in 2-D or 3-D. The basic building block of this scheme is the optimally accurate FD scheme for a region which is either homogeneous or has relatively mild velocity gradients. The operator for the general heterogeneous medium is then constructed by "overlapping" the operators for each of the regions (see, for example, Fig. 4, p.464, of Geller and Takeuchi, 1995). We present a numerical example. Fig. 3 shows a 2-D elastic P-SV model, and Fig. 4 shows synthetics computed for this model using the optimally accurate scheme of Takeuchi and Geller (2000).

DISCUSSION

As shown above, on the basis of both theory and numerical experiments, staggered-grid schemes are basically equivalent (but slightly inferior) to non-optimally accurate one-step schemes. If one looks at the history of FD methods, some of the early one-step "displacement only" schemes had substantial problems (instability, inability to handle internal discontinuities, free external boundaries, or gradients in material properties), and the use of staggered-grid methods in preference to the flawed one-step schemes was sensible. However, optimally accurate schemes (Geller and Takeuchi, 1998; Takeuchi and Geller, 2000; Hirabayashi *et al.*, 2006) do not suffer from the problems of earlier one-step schemes, while, as shown in this paper and elsewhere, optimally accurate schemes substantially outperform non-optimally accurate schemes. The use of optimally accurate schemes is thus clearly indicated, particularly in cases such as 3-D prestack reverse time migration, where computational accuracy and computational efficiency are important issues.

ACKNOWLEDGEMENTS

We thank Joe Stefani and Nozomu Takeuchi for helpful comments. This research was partly supported by grants from the Japan Society for the Promotion of Science (Nos. 17037001 and 17540392).

REFERENCES

Carcione, J. M., G. C. Herman, and ten A. P. E. Kroode, 2002, Seismic modeling: Geophysics: **67**, 1304–1325.

Claerbout, J. F., 1985, *Imaging the Earth's Interior*: Blackwell Scientific Publications.

Dablain, M. A., 1986, The application of high-order differencing to the scalar wave equation: Geophysics, **51**, 54–66.

Geller, R. J., and T. Ohminato, 1994, Computation of synthetic seismograms and their partial derivatives for heterogeneous media with arbitrary natural boundary conditions using the Direct Solution Method: Geophysical Journal International: **116**, 421-446.

Geller, R. J., and N. Takeuchi, 1995, A new method for computing highly accurate DSM synthetic seismograms, Geophysical Journal International: **123**, 449–470.

Geller, R. J., and N. Takeuchi, 1998, Optimally accurate second order time domain finite difference scheme for the elastic equation of motion: 1-D case, Geophysical Journal International: **135**, 48–62.

Geller, R. J., H. Mizutani, and N. Hirabayashi, 2006, Existence of a second range of stability of optimally accurate finite-difference schemes for numerically solving the wave equation: Journal of Computational Physics, submitted.

Hirabayashi, N., R. J. Geller, and H. Mizutani, 2006, Superiority of optimally accurate schemes for numerical calculation of synthetic seismograms: 1-D examples: Geophysical Journal International, submitted.

Kawai, K., N. Takeuchi, and R.J. Geller 2006, Complete synthetic seismograms up to 2 Hz for transversely isotropic spherically symmetric media, Geophysical Journal International: **164**, 411–424.

Kelly, K. R., R. W. Ward, S. Treitel, and R. M. Alford, 1976, Synthetic seismograms: A finite-difference approach: Geophysics, **41**, 2–27.

Korn, M., 1987, Computation of wavefields in vertically inhomogeneous media by a frequency domain finite-difference method and application to wave propagation in earth models with random velocity and density perturbations: Geophysical Journal of the Royal Astronomical Society, **88**, 345-377.

Lax, P. D., and B. Wendroff, 1964, Difference schemes for hyperbolic equations with high order of accuracy: Communications on Pure and Applied Mathematics, **17**, 381–398.

Levander, A. R., 1988, Fourth-order finite-difference seismograms: Geophysics: **53**, 1425–1436.

Luo, Y., and Schuster, G., 1990, Parsimonious staggered grid finite-differencing of the wave equation: Geophysical Research Letters, **17**, 155-158.

Marfurt, K. J., 1984, Accuracy of finite-difference and finite-element modeling of the scalar and elastic wave equations: Geophysics, **49**, 533-549.

Mizutani, H., 2001. *Accurate and Efficient Methods for Calculating Synthetic Seismograms when Elastic Discontinuities do not Coincide with the Numerical Grid*, D. Sc. Thesis, University of Tokyo.

Mizutani, H., and R. J. Geller, 2005, Stability of various free surface boundary conditions for time-domain finite-difference operators, paper presented at annual Joint Meeting of Japan Earth and Planetary Science Societies, Makuhari Messe, Japan, May 22-26, 2005.

Mizutani, H., R. J. Geller, and N. Takeuchi, 2000, Comparison of accuracy and efficiency of time-domain schemes for calculating synthetic seismograms: Physics of the Earth and Planetary Interiors, **119**, 75–97.

Strang, G. and G. J. Fix, 1973, *An Analysis of the Finite Element Method*: Prentice-Hall.

Takeuchi, N., and R. J. Geller, 2000, Optimally accurate second order time-domain finite difference

scheme for computing synthetic seismograms in 2-D and 3-D media: Physics of the Earth and Planetary Interiors, **119**, 99–131.

Takeuchi, N., and R. J. Geller, 2003, Accurate numerical methods for solving the elastic equation of motion for arbitrary source locations: Geophysical Journal International, **154**, 852-866.

Takeuchi, N., R. J. Geller, and P. R. Cummins, 1996. Highly accurate P-SV complete synthetic seismograms using modified DSM operators; Geophysical Research Letters, **23**, 1175-1178.

Virieux, J., 1984, SH-wave propagation in heterogeneous media—Velocity-stress finite-difference method: Geophysics, **49**, 1933-1957.

Virieux, J., 1986, P-SV wave propagation in heterogeneous media—Velocity-stress finite-difference method: Geophysics, **51**, 889-901.

APPENDIX

In this appendix we present a summary of key results for an optimally accurate $O(2,2)$ FD scheme (OPT2) at interior points of a homogeneous medium (after Geller and Takeuchi, 1998). We write the FD equation of motion in the time domain as follows:

$$(A_{mMnN} - K_{mMnN})\, c_{nN} = f_{mM}, \tag{37}$$

where **A** is the temporal FD operator and **K** is the spatial FD operator. We consider a homogeneous 1-D problem with a temporal grid interval Δt and a spatial grid interval Δx.

The format of the operators all follow that of **A**, as given below:

$$\mathbf{A} = \begin{array}{c|ccc} t+\Delta t & A_{(n-1)(N+1)nN} & A_{n(N+1)nN} & A_{(n+1)(N+1)nN} \\ t & A_{(n-1)NnN} & A_{nNnN} & A_{(n+1)NnN} \\ t-\Delta t & A_{(n-1)(N-1)nN} & A_{n(N-1)nN} & A_{(n+1)(N-1)nN} \\ \hline & x-\Delta x & x & x+\Delta x \end{array} . \tag{38}$$

We use the superscript $^{\mathbf{0}}$ to denote the conventional operators, which are as follows:

$$\mathbf{A^0} = \left(\frac{\rho}{\Delta t^2}\right) \times \begin{array}{c|ccc} t+\Delta t & & 1 & \\ t & & -2 & \\ t-\Delta t & & 1 & \\ \hline & x-\Delta x & x & x+\Delta x \end{array}$$

$$\mathbf{K^0} = \left(\frac{\mu}{\Delta x^2}\right) \times \begin{array}{c|ccc} t+\Delta t & & & \\ t & 1 & -2 & 1 \\ t-\Delta t & & & \\ \hline & x-\Delta x & x & x+\Delta x \end{array}, \tag{39}$$

where blank spaces in the FD stencils denote zeros.

Omitting the details of the derivation, the optimally accurate operators are found to be as follows:

$$\mathbf{A} = \left(\frac{\rho}{\Delta t^2}\right) \times \begin{array}{c|ccc} t+\Delta t & 1/12 & 10/12 & 1/12 \\ t & -2/12 & -20/12 & -2/12 \\ t-\Delta t & 1/12 & 10/12 & 1/12 \\ \hline & x-\Delta x & x & x+\Delta x \end{array}.$$

$$\mathbf{K} = \left(\frac{\mu}{\Delta x^2}\right) \times \begin{array}{c|ccc} t+\Delta t & 1/12 & -2/12 & 1/12 \\ t & 10/12 & -20/12 & 10/12 \\ t-\Delta t & 1/12 & -2/12 & 1/12 \\ \hline & x-\Delta x & x & x+\Delta x \end{array} \tag{40}$$

Note that if we sum horizontally for **A** and vertically for **K** we obtain the conventional operators

in eq. (39). An intuitive explanation of eq. (40) is that we smear out the discretized second time derivative operator in space, and smear out the discretized second spatial derivative operator in time, so that the numerical dispersion (error of the phase velocity) of the discretized equation of motion is zero to second order in Δt^2 and Δx^2.

The optimally accurate operator $(A_{mMnN} - K_{mMnN})$ given by eq. (40) has multiple non-zero elements for time $t + \Delta t$. If we use this operator in a time-marching scheme to solve eq. (37), we will have obtained an implicit scheme. To obviate the need to solve a system of simultaneous linear equations at each time step, we use a predictor-corrector scheme as follows. First we predict the wavefield at the next time step using the conventional operators $\mathbf{A^0}$ and $\mathbf{K^0}$ defined in eq. (39):

$$\left(\mathbf{A^0} - \mathbf{K^0}\right) \mathbf{c^0} = \mathbf{f}, \tag{41}$$

where c^0_{nN+1}, the predicted wavefield at time $t + \Delta t$, is obtained from eq. (41) by solving an explicit scheme.

Next we compute $\delta\mathbf{c}$, the correction to the displacement at time $t + \Delta t$, using the first order Born approximation. We denote the difference between the conventional operators $\mathbf{A^0}$, $\mathbf{K^0}$ and the modified operators $\mathbf{A}$, $\mathbf{K}$ by $\delta\mathbf{A}$, $\delta\mathbf{K}$ respectively. To obtain the correction we solve:

$$\left(\mathbf{A^0} - \mathbf{K^0}\right) \delta\mathbf{c} = -\left(\delta\mathbf{A} - \delta\mathbf{K}\right) \mathbf{c^0}, \tag{42}$$

where

$$\delta\mathbf{A} = \left(\frac{\rho}{\Delta t^2}\right) \times \begin{array}{|c|ccc|} \hline t+\Delta t & 1/12 & -2/12 & 1/12 \\ t & -2/12 & 4/12 & -2/12 \\ t-\Delta t & 1/12 & -2/12 & 1/12 \\ \hline & x-\Delta x & x & x+\Delta x \\ \hline \end{array} \tag{43}$$

$$\delta\mathbf{K} = \left(\frac{\mu}{\Delta x^2}\right) \times \begin{array}{|c|ccc|} \hline t+\Delta t & 1/12 & -2/12 & 1/12 \\ t & -2/12 & 4/12 & -2/12 \\ t-\Delta t & 1/12 & -2/12 & 1/12 \\ \hline & x-\Delta x & x & x+\Delta x \\ \hline \end{array} . \tag{44}$$

As the l.h.s. of eq. (42) uses the conventional operators, we can compute the value of $\delta\mathbf{c}$ at time $t+\Delta t$ by solving an explicit scheme. Note that $\delta c_{nN} = 0$ and $\delta c_{nN-1} = 0$ in eq. (42).

We compute the corrected displacement c_{nN+1} after each time step using $\mathbf{c^0}$ computed by eq. (41) and $\delta\mathbf{c}$ computed by eq. (42):

$$c_{nN+1} = c^0_{nN+1} + \delta c_{nN+1}. \tag{45}$$

Finally, before advancing to the next time step we redefine $\mathbf{c^0}$:

$$c^0_{nN+1} = c_{nN+1}. \tag{46}$$

Note that we use the displacements given by eq. (46) as the values for c^0_{nN} and c^0_{nN-1} in eq. (41) at subsequent time steps.

Numerical Recipe

The scheme for the predictor step is as follows:

$$\begin{aligned} c_n^{N+1} &= -c_n^{N-1} \\ &\quad + \left(\frac{\mu}{\rho}\frac{\Delta t^2}{\Delta x^2}\right) c_{n-1}^N \\ &\quad + \left(2 - \frac{2\mu}{\rho}\frac{\Delta t^2}{\Delta x^2}\right) c_n^N \\ &\quad + \left(\frac{\mu}{\rho}\frac{\Delta t^2}{\Delta x^2}\right) c_{n+1}^N \\ &\quad + \left(\frac{\Delta t^2}{\rho} F_n^N\right), \end{aligned} \tag{47}$$

where c_n^N and F_n^N are the displacement and the body force at x and t respectively, and c_n^{N+1} is the unknown displacement at $t + \Delta t$ to be determined; the other quantities in eq. (47) are all known.

The explicit discretized equation for the correction step (eq. 42) is as follows (note that $\delta c_n^N = \delta c_n^{N-1} = 0$):

$$\begin{aligned} \delta c_n^{N+1} &= \left(-\frac{1}{12} + \frac{\mu}{12\rho}\frac{\Delta t^2}{\Delta x^2}\right)\left[c_{n-1}^{N+1} - 2c_{n-1}^N + c_{n-1}^{N-1}\right] \\ &\quad + \left(\frac{2}{12} - \frac{2\mu}{12\rho}\frac{\Delta t^2}{\Delta x^2}\right)\left[c_n^{N+1} - 2c_n^N + c_n^{N-1}\right] \\ &\quad + \left(-\frac{1}{12} + \frac{\mu}{12\rho}\frac{\Delta t^2}{\Delta x^2}\right)\left[c_{n+1}^{N+1} - 2c_{n+1}^N + c_{n+1}^{N-1}\right] \end{aligned} \tag{48}$$

Finally, after computing δc_n^{N+1} for all nodes, and before proceeding to the next time step, we combine eqs. (48) and (47) to obtain the net (corrected) displacement:

$$c_n^{N+1} \leftarrow c_n^{N+1} + \delta c_n^{N+1}, \tag{49}$$

where we use $\leftarrow$ to denote a replacement rather than a mathematical equality.

Table 1. Stability limit and lowest order numerical dispersion

Scheme	$C <$	$\beta_{num} = \beta \times$
SG-2/CONV-2	1.000	$\left[1-(1-C^2)k^2\Delta x^2/24+\cdots\right]$
CONV-4	0.866	$\left[1+C^2k^2\Delta x^2/24+\cdots\right]$
SG-4	0.857	$\left[1+C^2k^2\Delta x^2/24+\cdots\right]$
OPT-2*	1.000	$\left[1-(4-5C+C^2)k^4\Delta x^4/720+\cdots\right]$
OPT-4*	1.031	$\left[1-C^4k^4\Delta x^4/720+\cdots\right]$

* These values are for the ordinary stability zone. There is also a second stability zone in the approximate range $1.2593 < C < 1.6279$ for OPT-4, and a second stability point at $C = 2$ for OPT-2 (see Geller *et al*., 2006, and Hirabayashi *et al*., 2006, for details).

Table 2. Exact dispersion relations

Scheme	$2A-2=$
SG-2/CONV-2	$C^2(2E-2)$
CONV-4	$(C^2/12)\ (-2F+32E-30)$
SG-4	$(C^2/576)\ (2G-108F+1566E-1460)$
OPT-2	$C^2(2E-2)+(6-8E+2F)(C^4/12-C^2/12)$
OPT-4	$(C^2/12)\ (-30+32E-2F)$
	$-(C^2/1080)\ (310-472E+200F-40G+2H)$
	$+(C^4/1728)\ (1414-1984E+632F-64G+2H)$

Note that $A=\cos\omega\Delta t$, $E=\cos k\Delta x$, $F=\cos 2k\Delta x$, $G=\cos 3k\Delta x$, and $H=\cos 4k\Delta x$.

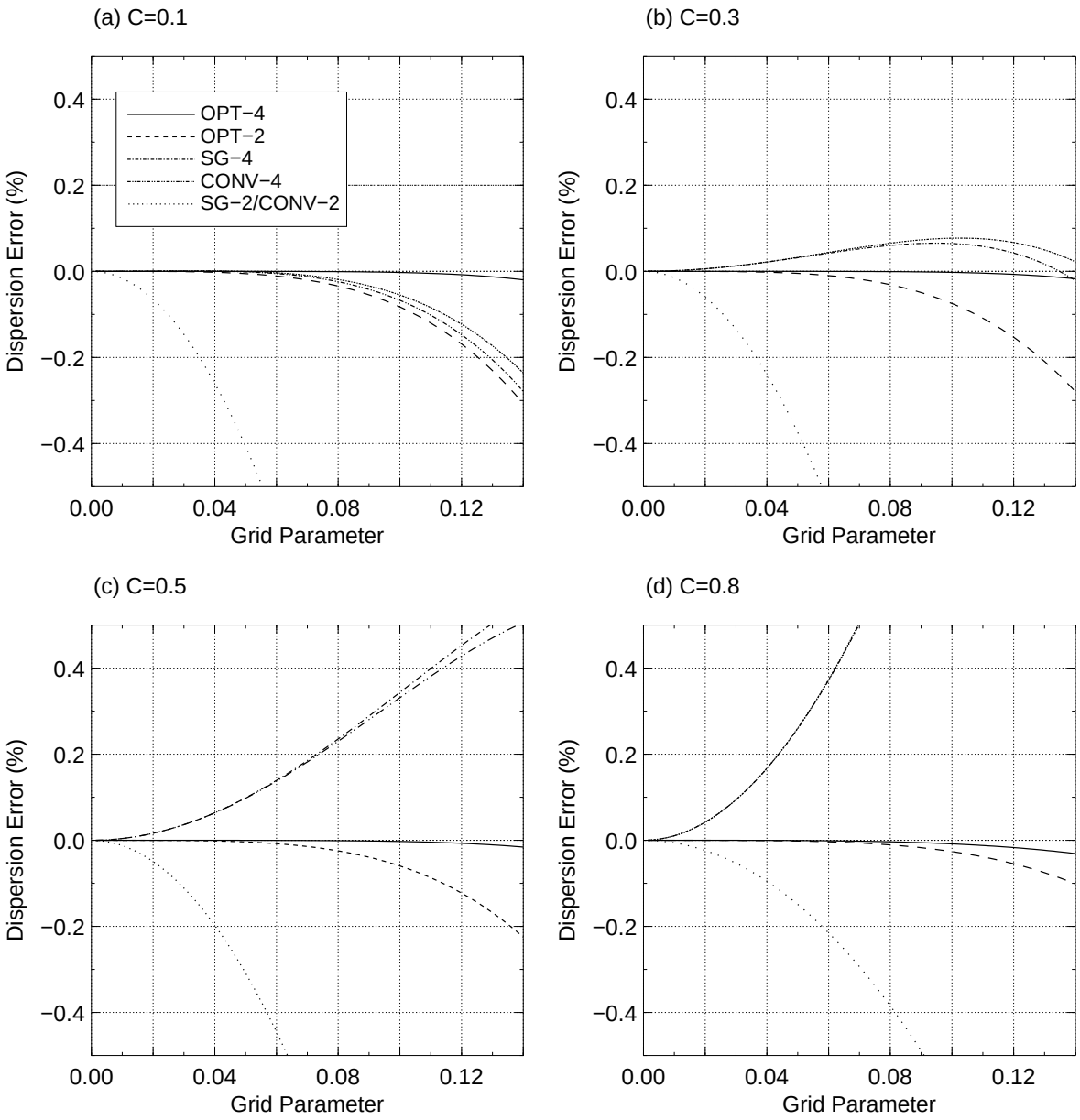

Figure 1: Numerical dispersion for the various schemes considered in this paper for four values of the Courant number (defined in eq. 29), $C = 0.1$, 0.3, 0.5, and 0.8. The horizontal axis is the grid parameter (number of grid intervals per wavelength), $\lambda/\Delta x = 2\pi/(k\Delta x)$. In almost all cases the optimally accurate schemes (OPT-2 and OPT-4) are significantly more accurate than the other schemes, but OPT-2 is comparable to CONV-4 and SG-4 for $C = 0.1$.

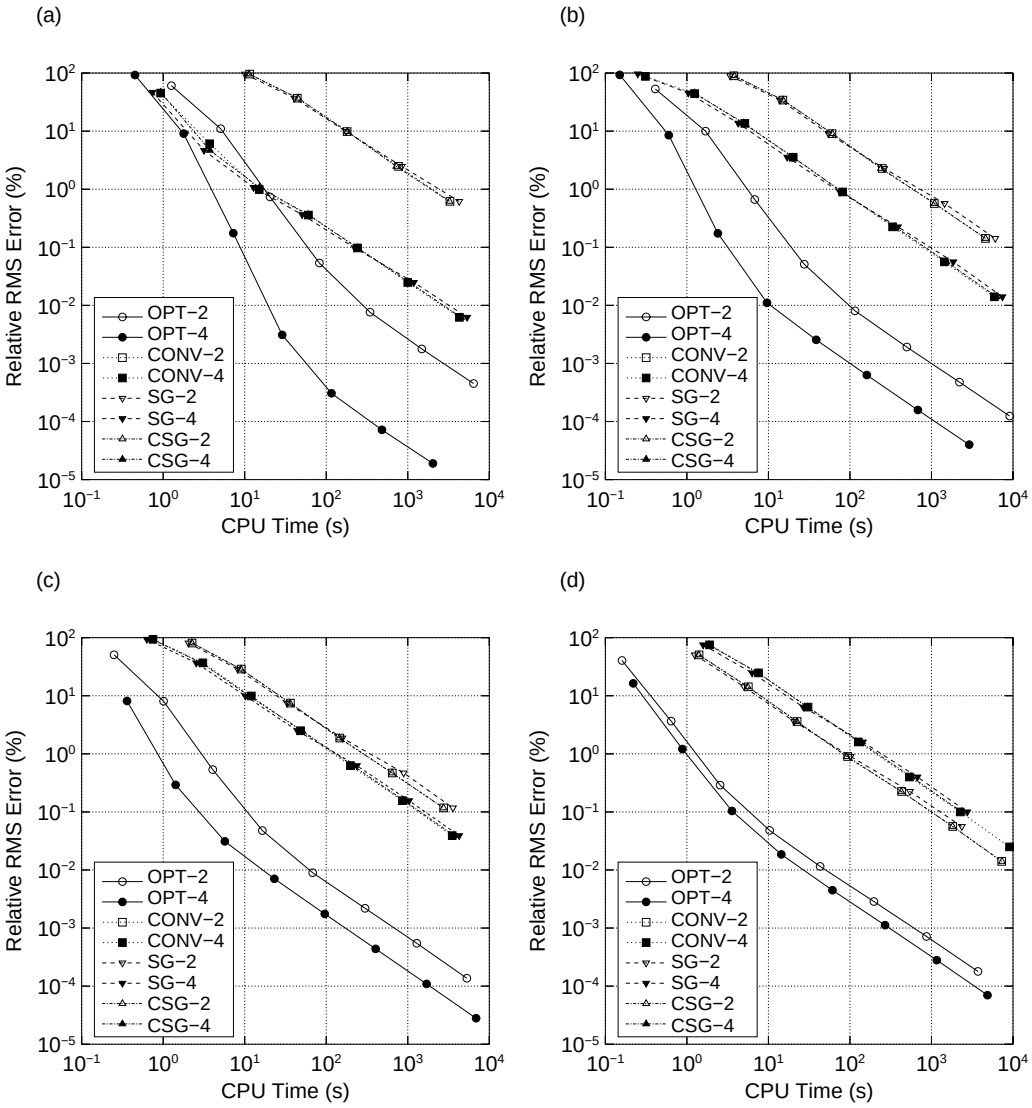

Figure 2: Tradeoff between CPU time and relative r.m.s. error for the various schemes considered in this paper for four values of the Courant number (defined in eq. 29): (a) $C = 0.1$, (b) $C = 0.3$, (c) $C = 0.5$, (d) $C = 0.8$. The schemes considered fall broadly into three classes: non-optimally accurate second order (SG-2, CONV-2, CSG-2), non-optimally accurate fourth order (SG-4, CONV-4, CSG-4), and optimally accurate (OPT-2 and OPT-4). The optimally accurate schemes significantly outperform all of the other schemes. There is no significant difference between staggered grid schemes and other non-optimally accurate schemes of the same order.

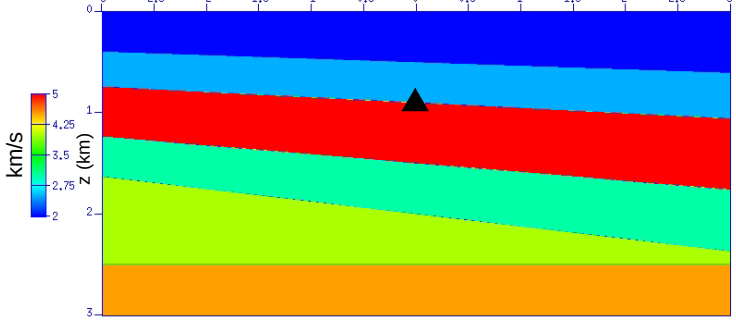

(a) Compressional velocity

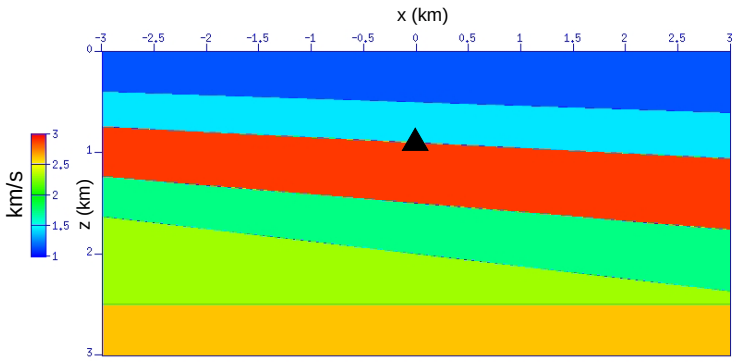

(b) Shear velocity

Figure 3: Heterogeneous 2-D elastic model used to generate the synthetic seismograms in Figure 4. The medium is a Poisson solid ($\lambda = \mu$). For simplicity a constant value of density was used, although our methods can handle arbitrarily heterogeneous density as well as arbitrarily heterogeneous elastic constants. The upper (a) and lower (b) figures show the P-wave velocity and the S-wave velocity respectively. The source (shown by the triangle) is a point force with Ricker wavelet time dependence and a center frequency of 25 Hz, applied at the interface between the second and the third layers, with force direction parallel to the interface. The grid spacing is constant throughout the medium. The number of grid points per wavelength (based on the slowest S-wave velocity) is 19.0 and the Courant number (based on the fastest compressional velocity) is $C = V_p \Delta t / \Delta z = 0.83$. The numerical operators at the boundaries are derived by "overlapping," as explained by Geller and Teakeuchi (1995) and Takeuchi and Geller (2000). Free surface conditions are imposed at all outer boundaries. Dipping interfaces at internal boundaries are approximated by stair-case boundaries.

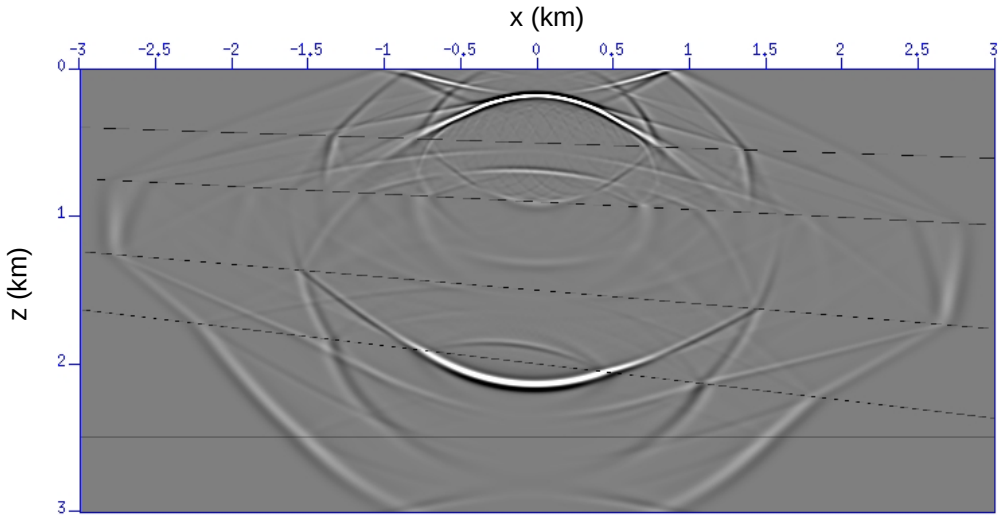

(a) Horizontal component

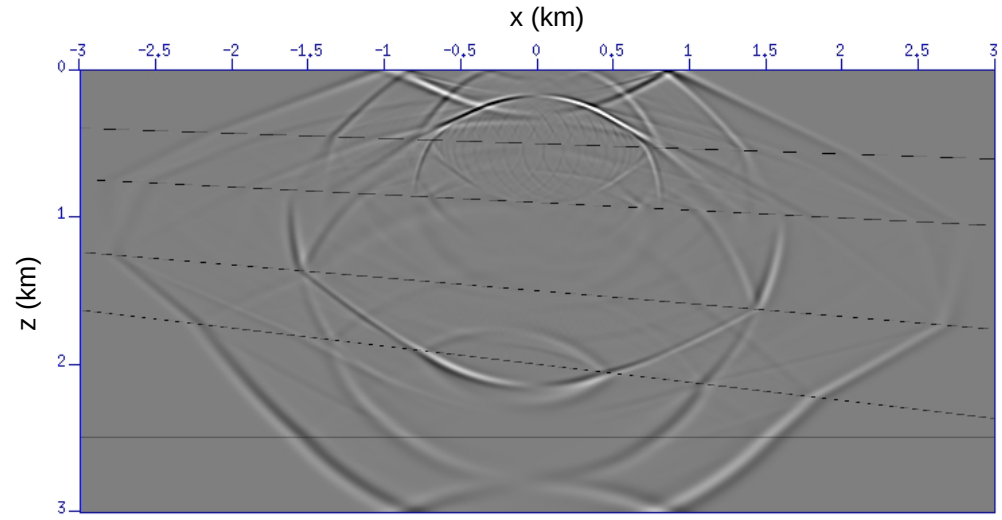

(b) Vertical component

Figure 4: Snapshots of P-SV synthetic seismograms for the 2-D model in Fig. 3: (a) the horizontal component and (b) the vertical component of the displacement at 0.6 (s) after the source is excited, computed using optimally accurate FD operators (Takeuchi and Geller, 2000).